Journal Name

COMMUNICATION

Silk fibroin nanoparticles as biocompatible nanocarriers of a novel light-responsive CO-prodrug

Received 00th January 20xx,
Accepted 00th January 20xx

DOI: 10.1039/x0xx00000x

www.rsc.org/

Ignacio Jiménez-Amezcua,[a†] Francisco J. Carmona,[a†] Ignacio Romero-García,[a] Miguel Quirós,[a] José L. Cenis,[b] A. Abel Lozano-Pérez,[b] Carmen R. Maldonado,*[a] Elisa Barea*[a]

$[Mn(CO)_3(2,2'\text{-bipyridine})(PPh_3)](ClO_4)$ (1), a novel photoactive CO-releasing molecule, has been prepared and fully characterized. Besides, silk fibroin nanoparticles (SFNs) have been used, for the first time, as vehicles of 1 leading to the hybrid material 1@SFNs that shows an enhanced CO-delivery.

During last decades, great efforts have been focused on the development of novel drug delivery systems (DDS).[1] DDS are designed to modify the biodistribution or pharmacokinetics of their associated bioactive compounds, to serve as drug reservoirs, or both.[2] Nanomaterials have emerged as promising carriers due to their unique features. In particular, they show tuneable particle size and morphology as well as high surface to volume ratio, which not only enables elevated drug payloads but also allows a wide variety of surface functionalizations, leading to highly specific receptor-targeting systems. Among them, silk fibroin (SF) from the silkworm *Bombix mori*, a protein based macromolecule comprising mainly Ala, Gly and Ser aminoacids,[3] has recently generated a great excitement in the field of biomedicine because its non-toxicity, biodegradability as well as non-thrombogenic, anti-inflammatory, cell-adhesive, cell-responsive and regenerative properties.[4,5] In particular, silk fibroin nanoparticles (SFNs) are the most promising SF-derived systems since they take advantage of both nanotechnology features and biocompatible silk-fibroin properties.[6] Indeed, SF nanoparticles have already demonstrated their utility as vehicles of several drugs or biomolecules, such as dextran or rhodamine B,[7] antitumoral platinum drugs,[8] and insulin,[9] among others.

On the other hand, carbon monoxide (CO) has emerged, in the last two decades, as an important biosignaling molecule, which exhibits many beneficial physiological effects (anti-inflammatory, antiproliferative, anti-apoptotic and antithrombotic) at low concentrations.[10] By contrast, this gasotransmitter has shown a bimodal role in carcinogenesis/tumorigenesis, as it displays a bell-shaped pharmacological behaviour that supports tumour growth and tumour angiogenesis at low concentrations while exerts cytotoxic effects at higher concentrations.[11] Regarding CO delivery systems, different macromolecular materials have been already explored as carriers of this therapeutic gas including polymeric organic and inorganic hybrid scaffolds, proteins, peptides and dendrimers.[12–16] In particular, our research group and others have recently developed several light-responsive CO-releasing materials (CORMAs)[17–21] based on inorganic porous solids, such as metal-organic frameworks and mesoporous silicas, and photoactive metal carbonyl complexes, known as photoCORMs. In spite of these few examples, CORMAs are still in their infancy and therefore, great efforts are still needed in order to achieve the real administration of exogenous CO for biomedical purposes. Taking into account this background, we report, herein, the synthesis and characterization, including X-ray single crystal structural studies, of the novel cationic tricarbonyl complex $[Mn(CO)_3(bpy)(PPh_3)](ClO_4)$ (**1**) (bpy = 2,2'-bipyridine; PPh_3 = triphenylphosphane). Besides, we have prepared and fully characterized a new CORMA based on the combination of silk fibroin nanoparticles (SFNs) and this CO-prodrug (**1@SFNs**). CO-releasing studies have revealed that both **1** and the hybrid

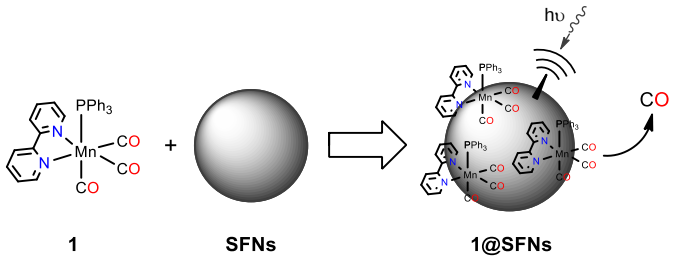

Scheme 1. Biocompatible CORMA based on silk fibroin nanoparticles and the photo-active CORM $[Mn(CO)_3(bpy)(PPh_3)]ClO_4$ (**1**).

[a] *Departamento de Química Inorgánica, Universidad de Granada, Av. Fuentenueva S/N, 18071 Granada, Spain.*
[b] *Departamento de Biotecnología, Instituto Murciano de Investigación y Desarrollo Agrario y Alimentario (IMIDA). La Alberca (Murcia), 30150, Spain.*
† I. Jiménez-Amezcua and F. J. Carmona equally contributed to this work.

Electronic Supplementary Information (ESI) available: SEM image of silk fibroin nanoparticles (SFNs), TG of $[Mn(CO)_3(bpy)(PPh_3)](ClO_4)$ (**1**), EDX-TEM of hybrid **1@SFNs**, storage stability tests of **1@SFNs**, screening of drug loading by ICP-MS, experimental section and detailed X-ray diffraction data. See DOI: 10.1039/x0xx00000x.

material **1@SFNs** behave as CO delivery agents, upon irradiation with visible light, with **1@SFNs** exhibiting an improved CO release in comparison to the free manganese complex (Scheme 1).

Silk fibroin nanoparticles (SFNs) were prepared following an adapted version of the firstly reported method by Zhang et al. (see ESI).[22,23] The obtained nanoparticles were repeatedly washed with ultrapure water, recovered by centrifugation and, finally, resuspended in water at 20 mg/mL until use. SFNs were characterized by scanning electron microscopy (SEM) and dynamic light scattering (DLS). SEM images showed spherical nanoparticles of about 100 nm while DLS studies revealed that SFNs show a good dispersion in aqueous solution (hydrodynamic size: 159.2 ± 0.3 nm, PdI: 0.07 ± 0.01) (Figure S1). In addition, the presence of negatively charged amino acid residues[24] on the surface of these nanoparticles (*Z*-potential: -24.6 ± 0.6 mV) may facilitate their interaction with different cationic molecules. Moreover, it is expected that aromatic moieties in the drug skeleton may favor its immobilization by interaction with the hydrophobic regions of the SF β-sheets.[3] Taking into account these considerations, and in order to optimize the interaction between the CO-prodrug and the SF carrier, we have designed and synthetized the cationic manganese compound $[Mn(CO)_3(bpy)(PPh_3)](ClO_4)$ (**1**) (bpy = 2,2'-bipyridine; PPh_3 = triphenylphosphane). For this purpose, the previously reported $[Mn(CO)_3(bpy)Br]$[25] was transformed into $[Mn(CO)_3(bpy)(solv)]ClO_4$, which was later reacted with an excess of triphenylphosphane at room temperature leading to the final manganese complex **1.** The as-synthetized compound was recrystallized in dichloromethane-ethanol solution giving rise to orange crystals suitable for single X-ray diffraction analysis.§ The recrystallized compound was also analyzed by elemental analysis, infrared spectroscopy and thermogravimetry (see ESI and Figure S2). The crystal structure of **1** is made up of discrete octahedral $[Mn(CO)_3(bpy)(PPh_3)]^+$ cations, exhibiting roughly a Cs symmetry,‡ and interstitial perchlorate counterions (Figure 1). The bpy ligand adopts its usual chelating mode while the other ligands display a monodentate fashion with CO moieties in *fac* disposition. Mn-C and C-O distances are as expected for manganese carbonyl complexes, with the Mn-C distance *trans* to P being somewhat longer than those *trans* to N. This fact can be attributed to the stronger π-acceptor character of the phosphane ligand, which hinders back Mn → C donation for the *trans* CO (see ESI). In addition, a clear π-stacking intramolecular interaction takes place between one of the pyridine rings of bpy (that containing N10B) and one of the phenyl rings of PPh_3 (that containing C21A) with a distance between the respective centroids of 3.51 Å. In contrast, this is not observed for the other bpy ring as this intramolecular interaction would probably imply a sterically hindered conformation for PPh_3. Finally, crystal packing is governed by usual Van der Waals interactions, which include: *i)* some C(phenyl)-H ··· O(perchlorate or CO) contacts (C ··· O distances 3.2-3.4 Å) that may be regarded as weak hydrogen bonds and *ii)* the interaction between one of perchlorate oxygens and the central carbons of bpy moieties (distance O ··· C ~ 3.0 Å).

Once both CO-prodrug and silk fibroin carrier were fully characterized, we screened different loading ratios and incubation periods in order to select the optimal experimental conditions to successfully adsorb **1** in the above mentioned nanoparticles. With this aim, suspensions of SFNs (1, 5 and 10 mg/mL) were incubated, in MeOH:H_2O (1:1) during 30 min, with a fixed CORM concentration (0.1 mg/mL) leading to mixtures with CORM/SFNs ratios of 1/10, 1/50 and 1/100, respectively. Afterwards, the pellets were collected by centrifugation, washed three times with MeOH:H_2O and dried under nitrogen flow. In order to quantify CORM loading, manganese was analyzed by ICP-MS. The results were expressed in terms of final drug cargo (Table S1). Regarding the former, CORM loading significantly decreases (~50%) when passing from 1/10 to 1/50 CORM/SFNs ratios (1.18 and 0.60 mg of **1** per 100 mg of material, respectively), while smaller changes were observed when comparing 1/50 and 1/100 ratios (0.60 and 0.48 mg of **1** per 100 mg of material, respectively). Besides, drug cargo did not improve substantially when longer incubation periods (1 and 3 h) were assayed for 1/50 CORM/SFNs ratio (Table S1). Additionally, and in order to evaluate the impact that the presence of PPh_3 and the cationic nature of **1** may exert on the final drug cargo (see above), we performed a control experiment by loading the neutral precursor $[Mn(CO)_3(bpy)Br]$ on SFNs. ICP-MS data confirmed that, in this case, a lower cargo was obtained (Table S2). In fact, the CORM loading in the SFNs was enhanced when **1** was used instead of $[Mn(CO)_3(bpy)Br]$ (31%, 46% and 45% of

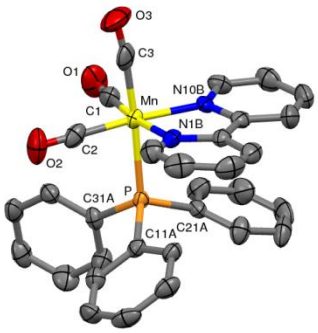

Figure 1. Crystal structure of the cationic CORM $[Mn(CO)_3(bpy)(PPh_3)]^+$. Hydrogens have been omitted for the sake of clarity. C: grey; N: blue; O: red; P: orange, Mn: yellow.

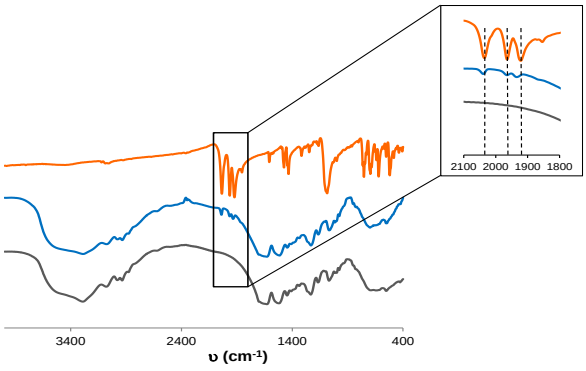

Figure 2. Infrared spectra of free $[Mn(CO)_3(bpy)(PPh_3)]ClO_4$ (**1**) (orange), SFNs (grey), and hybrid material **1@SFNs** (blue). The inset shows the displacement of the CO stretching bands in the hybrid material in comparison to the free CORM.

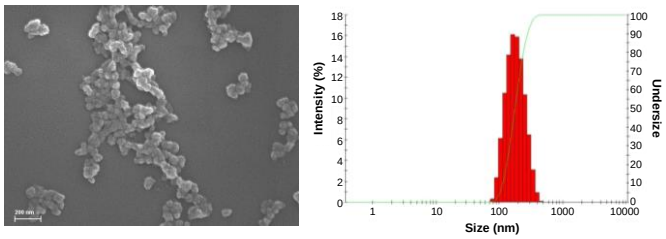

Figure 3. SEM image (left) and DLS size distribution profile (right) of **1@SFNs**.

increase for 1/10, 1/50 and 1/100 ratios, respectively). In view of these results and taking into account the better affinity of the cationic moiety $[Mn(CO)_3(bpy)(PPh_3)]^+$ for SNFs, we selected complex **1** as a suitable candidate to prepare a novel light responsive CO prodrug based on SFNs. Particularly, 1/10 ratio and 30 minutes of incubation were selected as the optimal experimental conditions for the scale-up synthesis of the hybrid material **1@SFNs**. The successful loading of complex **1** into SFNs was confirmed by EDX-TEM (Figure S3), IR spectroscopy and quantified again by ICP-MS (Table S1). Regarding IR spectra, two of the characteristic stretching CO bands of **1** appear slightly shifted in the loaded SFNs (2039, 1964, 1933 cm^{-1}) in comparison with the free CORM (2035, 1964, 1921 cm^{-1}) (Figure 2), which may be attributed to the interaction between the cationic CORM moiety and the negatively charged silk nanoparticles surface. In addition, quantitative IR spectroscopy assessed the stability of the hybrid material when stored in the solid state at 4 °C and in darkness (Figure S4). Indeed, no changes in characteristic CO stretching bands intensity were observed even after three months. The hybrid system was further characterized by SEM and DLS. As shown in Figure 3, **1@SFNs** exhibited similar size and morphology in the solid state than unloaded SFNs (Figure S1). Furthermore, hydrodynamic size was quite similar to that of unloaded SF nanoparticles confirming the good dispersion of the hybrid material (163.9 ± 4 nm; PdI: 0.15 ± 0.02) (Figure 3).

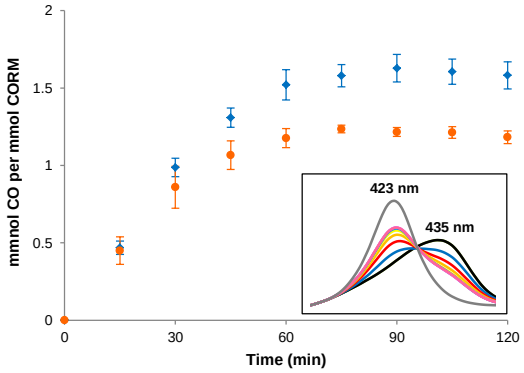

Figure 4. CO releasing kinetics upon irradiation with visible light of free CORM (**1**) (orange dots) and the hybrid material **1@SFNs** (blue diamonds). The inset shows the evolution of the electronic spectra of myoglobin upon CO coordination. Experimental conditions: Ar atmosphere, 10 mM PBS, 37 °C, 2 µM of **1** and 6 µM of myoglobin.

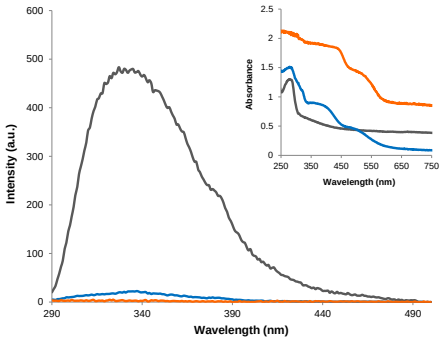

Figure 5. Solid-state fluorescence spectra of silk fibroin nanoparticles (grey), $[Mn(CO)_3(bpy)(PPh_3)]ClO_4$ (**1**) (orange) and hybrid system **1@SFNs** (blue) (λ_{exc} = 280 nm). The inset shows the corresponding reflectance diffuse spectra.

Finally, we evaluated the suitability of free **1** and the hybrid system **1@SFNs** for the controlled delivery of CO under simulated physiological conditions (PBS 10 mM, 37 °C). In order to monitor this CO release we selected the well-established myoglobin assay.[26,27] When kept in dark, neither **1** nor **1@SFNs** show any spectral changes over 3 h. In contrast, upon irradiation with visible light (luminous flux, 600 lm; color temperature, 4000 K, distance between lamp and cuvette, 5 cm), photoactivation occurs as spectral changes characteristic of CO binding to the myoglobin iron center were observed in both cases (Figure 4). Indeed, **1** released 1.18 ± 0.04 mmol of CO per mmol of complex after 120 min, confirming the higher lability of one of the three CO ligands per complex. Noteworthy, although the hybrid system **1@SFNs** retains the photoactivable properties of free CORM and shows a similar CO kinetic profile, a higher amount of delivered CO was observed (1.58 ± 0.09 mmol of CO per mmol of complex after the same time frame). Fluorescence studies revealed that, when the hybrid material was excited at 280 nm, the intrinsic silk fibroin fluorescence at 380 nm was quenched (Figure 5). This result might be indicative of a charge transfer process from SFNs to the attached manganese complex, and consequently related to the more efficient labilization of the corresponding CO ligands.

Conclusions

In this work, we have prepared and characterized by single X-ray crystal diffraction the new CO-releasing molecule $[Mn(CO)_3(bpy)(PPh_3)](ClO_4)$ (**1**). This tricarbonyl complex behaves as a photoCORM, upon irradiation with visible light, releasing *ca*. one CO per manganese unit. The loading of this CORM on silk fibroin nanoparticles has been successfully achieved by simple adsorption, leading to the first example of a light responsive CO-prodrug system based on biocompatible silk fibroin nanocarriers (**1@SFN**). Noteworthy, this hybrid material releases approximately 34 % more of CO compared to free CORM, which is related to a more efficient CO ligand sensitization of the manganese complex attached to the silk fibroin nanoparticles.

Conflicts of interest

There are no conflicts to declare.

Acknowledgements

The Spanish Ministry of Economy and Competitivity and UE Feder Program (CTQ2017-84692-R), University of Granada (C. R. Maldonado, Reincorporación Plan Propio, I. Romero-García, Beca de Iniciación a la Investigación Plan Propio and Unidad de Excelencia "Química Aplicada a Biomedicina y Medioambiente"), ERDF/FEDER Operative Programme of the Region of Murcia (Project No. 14-20-01) are gratefully acknowledged for generous funding. The research contract of Dr. A. Abel Lozano-Pérez was partially supported (80%) by the ERDF/FEDER Operative Programme of the Region of Murcia (Project No. 14-20-01). Authors also thank Prof. Meseguer-Olmo and Dr. M. J. Yáñez-Gascón (UCAM, Murcia, Spain) for their help during FESEM images acquisition.

Notes and references

§ Crystal Data for **1**: $[Mn(CO)_3(bpy)(PPh_3)](ClO_4)$, M = 656.87, monoclinic, space group P21/n, a = 10.5698(4), b = 21.1564(9), c = 12.7711(5) Å, β = 100.017(1)°, V = 2812.33(19) Å^3, Z = 4, D_{calc} = 1.551 g cm^{-3}, T = 100 K, MoK_α = 0.71073 Å, R_{int} = 0.0733, R(F, $F^2 > 2\sigma$) = 0.0505, $R_w(F^2$, all data) = 0.0954 for 7076 unique reflections, goodness-of-fit = 1.023. CCDC 1827124.
‡ Neglecting differences in phenyl ring conformation.

1 K. Park, *J. Control. Release*, 2014, **190**, 3–8.
2 T. M. Allen and P. R. Cullis, *Science*, 2004, **303**, 1818–1822.
3 Y. X. He, N. N. Zhang, W. F. Li, N. Jia, B. Y. Chen, K. Zhou, J. Zhang, Y. Chen and C. Z. Zhou, *J. Mol. Biol.*, 2012, **418**, 197–207.
4 F. G. Omenetto and D. L. Kaplan, *Science,* 2013, **528**, 528–532.
5 A. B. Mathur and V. Gupta, *Nanomedicine*, 2010, **5**, 807–820.
6 F. Mottaghitalab, M. Farokhi, M. A. Shokrgozar, F. Atyabi and H. Hosseinkhani, *J. Control. Release*, 2015, 206, 161–176.
7 X. Wang, T. Yucel, Q. Lu, X. Hu and D. L. Kaplan, *Biomaterials*, 2010, **31**, 1025–1035.
8 A. A. Lozano-Pérez, A. L. Gil, S. A. Pérez, N. Cutillas, H. Meyer, M. Pedreño, S. D. Aznar-Cervantes, C. Janiak, J. L. Cenis and J. Ruiz, *Dalt. Trans.*, 2015, **44**, 13513–13521.
9 H. B. Yan, Y. Q. Zhang, Y. L. Ma and L. X. Zhou, *J. Nanoparticle Res.*, 2009, **11**, 1937–1946.
10 R. Motterlini and L. E. Otterbein, *Nat. Rev. Drug Discov.*, 2010, **9**, 728–743.
11 C. Szabo, *Nat. Rev. Drug Discov.*, 2016, 15, 185–203.
12 D. Nguyen and C. Boyer, *ACS Biomater. Sci. Eng.*, 2015, **1**, 895–913.
13 A. C. Kautz, P. C. Kunz and C. Janiak, *Dalt. Trans.*, 2016, **45**, 18045–18063.
14 H. Inaba, K. Fujita and T. Ueno, *Biomater. Sci.*, 2015, **3**, 1423–1438.
15 X. Ji, K. Damera, Y. Zheng, B. Yu, L. E. Otterbein and B. Wang, *J. Pharm. Sci.*, 2016, **105**, 406–415.
16 I. Chakraborty and P. K. Mascharak, *Microporous Mesoporous Mater.*, 2016, **234**, 409–419.
17 F. J. Carmona, S. Rojas, C. Romao, J. A. R. Navarro, E. Barea and C. R. Maldonado, *Chem. Commun.*, 2017, **53**, 6581–6584.
18 F. J. Carmona, I. Jiménez-Amezcua, S. Rojas, C. C. Romão, J. A. R. Navarro, C. R. Maldonado and E. Barea, *Inorg. Chem.*, 2017, **56**, 10474–10480.
19 F. J. Carmona, S. Rojas, P. Sánchez, H. Jeremias, A. R. Marques, C. C. Romão, D. Choquesillo-Lazarte, J. A. R. Navarro, C. R. Maldonado and E. Barea, *Inorg. Chem.*, 2016, **55**, 6525–6531.
20 I. Chakraborty, S. J. Carrington, J. Hauser, S. R. J. Oliver and P. K. Mascharak, *Chem. Mater.*, 2015, **27**, 8387–8397.
21 S. Diring, A. Carné-Sánchez, J. Zhang, S. Ikemura, C. Kim, H. Inaba, S. Kitagawa and S. Furukawa, *Chem. Sci.*, 2017, **8**, 2381–2386.
22 Y. Q. Zhang, W. De Shen, R. L. Xiang, L. J. Zhuge, W. J. Gao and W. B. Wang, *J. Nanoparticle Res.*, 2007, **9**, 885–900.
23 A. A. Lozano-Pérez, H. C. Rivero, M. del C. Pérez Hernández, A. Pagán, M. G. Montalbán, G. Víllora and J. L. Cénis, *Int. J. Pharm.*, 2017, **518**, 11–19.
24 A. S. Lammel, X. Hu, S. H. Park, D. L. Kaplan and T. R. Scheibel, *Biomaterials*, 2010, **31**, 4583–4591.
25 R. Usón, V. Riera, J. Gimeno and M. Laguna, *Transit. Met. Chem.*, 1977, **2**, 123–130.
26 R. Motterlini, J. E. Clark, R. Foresti, P. Sarathchandra, B. E. Mann and C. J. Green, *Circ. Res.*, 2002, **90**, e17–e24.
27 D. E. Bikiel, E. G. Solveyra, F. Di Salvo, H. M. S. Milagre, M. N. Eberlin, R. S. Corrêa, J. Ellena, D. A. Estrin and F. Doctorovich, *Inorg. Chem.*, 2011, **50**, 2334–2345.

